

Simulation of operating loads of ablative composite shields used in flight data recorders

Pawel Przybyłek¹, Tadeusz A. Opara², Wojciech Kucharczyk², Wojciech Żurowski², Agata Pietras³

¹ Military University of Aviation, Faculty of Aviation, Poland, e-mail: p.przybylek@law.mil.pl

² Kazimierz Pulaski University of Technology and Humanities in Radom, Faculty of Mechanical Engineering, Poland, e-mail: t.opara@uthrad.pl, wojciech.kucharczyk@uthrad.pl, wojciech.zurowski@uthrad.pl

³ Military University of Technology, Faculty of Mechatronics And Aviation, Poland, e-mail: agata.pietras@hotmail.com

Article Info

Article history:

Received January 3, 2022

Revised March 11, 2022

Accepted March 14, 2022

Keywords:

Thermo-protective shields,
Flight data recorders,
Endurance tests of recorder covers,
Mathematical modeling,
Numerical simulation.

ABSTRACT

The objects of the mathematical simulation were two covers of the same shape, but different geometrical dimensions. The covers were made of aramid fabric, alternating and uniformly distributed in the composite - in a polymer matrix of epoxy resin, modified with 15% addition of MMT. For each of the two guards, four variants of the composite material were considered in correlation with the metal casing, as well as three load cases, in accordance with the normative documents. A numerical analysis of dynamic tests was performed to determine the durability of the recorder. As a result of the conducted analyses, stress values were obtained in all load cases and for all kinds of placement of the composite in correlation with the metal reinforcement casing. The displacements of the entire model and stress σ_x were analyzed as a possible cause of delamination, while the shear stress τ_{yz} is a possible cause of inter-cutting. Also, a detailed distribution of stresses reduced in subsequent layers of the cover material was analyzed. The distribution of kinetic and potential energy during piercing of the composite thermo-protective casing was determined by numerical simulation and the design of the recorder housing made of an epoxy ablation composite, with a metal casing located inside the casing, was considered.

Copyright © 2022 Regional Association for Security and crisis management and European centre for operational research.
All rights reserved.

Corresponding Author:

Wojciech Kucharczyk,
Kazimierz Pulaski University of Technology and Humanities in Radom, Poland
Email: wojciech.kucharczyk@uthrad.pl

1. Introduction

The term ablation refers to the exchange of heat and mass in the body's upper layer in thermochemical and mechanical processes. There are many technical applications for ablative material. Polymeric ablation materials are increasingly used in the field of thermal protection systems. They can be used in the design of passive refractories for load-bearing structures of large-size buildings (NIST NCSTAR 1, 2005); Wilkinson, 2002), communication tunnels (Haack, 2004; Ono & Otsuka, 2006) and for protection of data stored on electronic, optical, magnetic, etc.

Good protective properties in buffering of fire and thermal shock can be obtained using composite polymer coverings with typical ablative composite matrices like silicone resin (Yuan et al., 2018), phenol resins (Kucharczyk et al., 2013; Pulci et al., 2010; Bahramian, 2013; Zhou et al., 2019) or epoxy resins (Kucharczyk, 2010; Bakar et al., 2016; Camino et al., 2005; Kucharczyk et al., 2018; Krzyżak et al., 2018; Stawarz et al., 2019) with fillers that increase the thermal stability of a composite. Pure resins are good ablative materials. They require reinforcement (Xie et al., 2020), however, due to their low decomposition temperature, porosity and fragility of the ablative layer (Rallini et al., 2018). Addition of powders (Yuan

et al., 2018; Kucharczyk et al., 2013; Bakar et al., 2016; Camino et al., 2005; Lombardi et al., 2012; Fino et al., 2012), nanopowders (Stawarz et al., 2019) or fibre reinforcement (Pulci et al., 2010; Bahramian, 2013; Kucharczyk, 2010; Xie et al., 2020; Alagar et al., 2000; Minkook et al., 2016) or reinforcing plates (Yuan et al., 2018; Fino et al., 2012; Shi et al., 2020) of high melting temperatures build a composite structure that substantially improves thermoprotective, thermomechanical (Shi et al., 2020) and mechanical (Xie et al., 2020; Bieniaś & Jakubczak, 2017) properties of a polymer ablative composite.

Flight Data Recorders (FDR) (Ministere des Transports, 2005; EUROCAE, 2013; Polak & Rypulak, 2002; Przybyłek & Opara, 2010) are designed to record the main flight parameters and operational parameters of the work of aircraft assemblies for evaluation (NHTSA, 2010; NHTSA, 2015): flight safety, piloting techniques, the status of on-board systems, causes of an accident or plane crash.

In addition, the recorders of operation parameters of various operational objects are increasingly used by car manufacturers (ADAC, 2015; GM, 2016; IEEE 1616, 2004), locomotives, ships, and even architecture, in order to assist all emergency services involved in removing the consequences, and then determining the causes of the existing communication (building) disasters. Usually it is a measurement and diagnostic module SDM (Sensing and Diagnostics Module), from which information is read and archive during technical inspections. They support the diagnostic process and enable to analyze the causes of faults. It is the basis for modifying procedures used when locating disabilities and determining selected reliability indicators.

Requirements for registrars concern many different aspects of their exploitation. The most important criterion was the possibility of recovering archived information.

The construction of the protective casing must ensure resistance to a number of factors causing accidents or disasters (Tab. 1).

Table 1. Quality requirements for the protection of recorded information (Przybyłek & Opara, 2010).

| Requirement | Flight Data Recorders | Railway recorder | Data registration systems for building objects |
|--|---|---|---|
| Impact loading | 3400/6.5 ms | 23 g/250 ms or energy equivalent | ----- |
| Puncture resistance | 10 ft. drop 500 lbs., 0.05 in ² (mass ~ 227 kg dropped from ~3 m) | Not required | Mass 227 kg dropped from a height 3 m ~1.2 m |
| Static load | 5,000 lbf/5 min., surface and slanted (~2268 kg/5 min) | 25,000 lbf/5 min., on the entire surface (~11340 kg/5 min.) | 25,000 lbf/5 min. (~7620 m/5 min.) |
| Head crush | Not required | 10,000 lbf/5 min. on the 25% surface (~4536 kg/5 min) | Not required |
| Flame, high temperature heat flux | 1100°C, 60 min. | 1000°C, 60 min. | 1200°C, 60 min. |
| Low-temperature heat flux | 260°C, 10 hours | 260°C, 10 hours | 260°C, 10 hours |
| Immersion in fuel /operating fluids | 48 godz. | 48 hours | 48 hours |
| Immersion in sea water | 9 ft/30 days (~3 m/30 days) | 48 hours | Not required |
| Immersion in extinguishing media | 8 hours | 48 hours | 8 hours |
| Hydrostatic pressure | 20 000 ft/30 days (6000 m/30 days) | 48 hours | Not required |

To determine the full ability of a universal thermo-protective cover to protect the recorder's data carriers after an accident or disaster, all tests described in Table 1 should be performed. Endurance tests of recorder covers are very destructive, causing damage to them, and even complete desolation during the tests. Test of resistance to static load involves checking the strength of the protective housing subjected to a force of 22.25 kN for 5 minutes, along specific directions for a given shape. Their implementation requires the design and execution of a measurement station and the production of a series of covers that will be subjected to strength tests. These are usually destructive tests. A complementary method of strength analysis is mathematical

modeling. Software supporting engineering design allows you to conduct model tests with a much smaller amount of funds and analysis of various configurations, dimensions and method of spreading the laminate sheath on the housing material of the flight recorder (Ryabov et al., 2003). The ANSYS 15.0 software was used for numerical analysis of dynamic loads of guards.

2. Mathematical modeling

Two covers with the same shape but different sizes (Tab. 2 and Fig. 1) were selected for the model tests. The wall thickness of the model (cover) was 12.65 mm (Przybyłek, 2018).

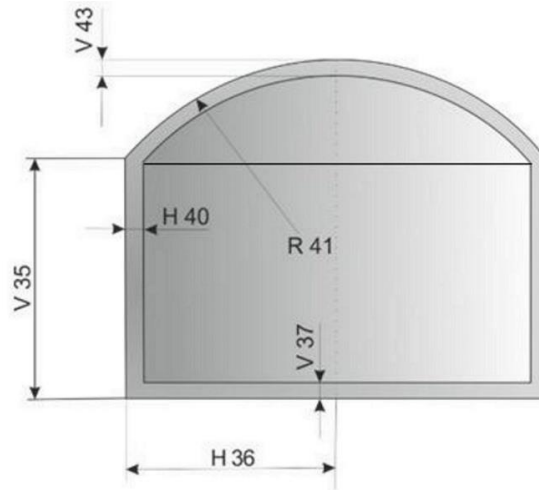


Figure 1. The shape and dimensions of the composite shell.

The objects of the mathematical simulation were two covers of the same shape, but different geometrical dimensions. The protective covers were made of the following components: 14 layers of aramid fabric with a weight of 230 g/m², alternating and uniformly distributed in the composite - in a polymer matrix of *Epidian 52* epoxy resin, crosslinked *TFF* hardener, modified with 15% addition of layered aluminosilicate *Bentonit Specjal Extra* with 75% content of calcium montmorillonite *MMT* (Przybyłek, 2018).

The following cases were considered for both covers:

1. The housing of the flight recorder is the cover made only of ablative polymer composites.
2. Cover made of ablative polymer composites is placed outside the metal housing of flight recorder.
3. Cover made of ablative polymer composites is placed inside the metal housing of flight recorder.
4. Cover made of ablative polymer composites is placed inside and outside the housing of the flight recorder, in a way that its total thickness is the same as in the case of the two previous variants.

Table 2. Dimensions of thermo-protective covers (Przybyłek, 2018).

| | Cover 1, (mm) | Cover 2, (mm) | | |
|-----|---------------|---------------|--------|--|
| H36 | 135 | H40 | 12.65 | |
| H40 | 12.65 | H45 | 21.5 | |
| R41 | 172.69 | R41 | 175.09 | |
| V35 | 153 | V35 | 135 | |
| V37 | 12.65 | V37 | 12.65 | |
| V43 | 12.65 | --- | --- | |

Due to the way the sample is made for experimental tests of a composite cover the numerical model was adopted consisting of three permanently connected elements: groundwork, cylinder and bowl (Fig. 2).

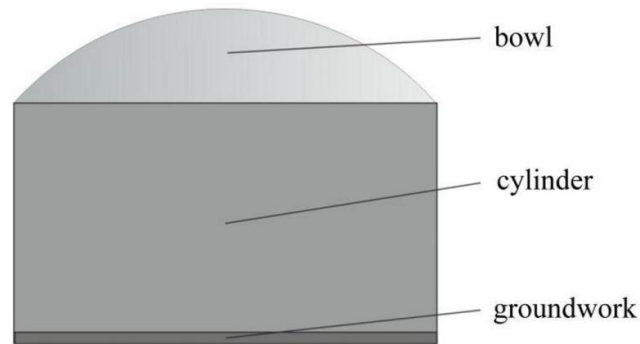


Figure 2. Numerical 3D model divided into individual elements of a composite cover.

The modeled object was divided into finite elements Tet10 and Hex20. Numerical calculations were carried out for the assumed boundary conditions and loads. The mass and volume fractions of carbon fiber f_w and aramid f_c were also determined (Tab. 3).

Table 3. Values of mass and volume share of fibers and matrix in epoxy composites (Przybyłek, 2018).

| Mass shares of reinforcement and matrix in laminate | | |
|---|--------------------------|-------------------------|
| Carbon fiber m_w , (%) | Aramid fiber m_A , (%) | Epoxy resin m_o , (%) |
| 7.24 | 24.3 | 68.46 |
| Volume shares of the reinforcement and matrix in the laminate | | |
| 7.04 | 27.06 | 65.9 |

According to normative documents (14 CFR § 121.344, 2011), each of the modeled covers has been subjected to the following loads:

1. A concentrated force of 22 250 N on the square surface (38.5 mm × 38.5 mm for the cover from an epoxy ablation composite and 25.0 mm × 25.0 mm for layers arranged on the metal surface of the recorder housing), directed towards the y axis (compression) (Fig. 3).
2. A concentrated force of 22 250 N on the node of the edge connecting the bowl with the cylinder, directed at an angle of 45° (Fig. 4).
3. A concentrated force of 22 250 N on the surface of the rectangle (12.55 mm × 7.0 mm for the cover from an epoxy ablation composite, 5.00 mm × 7.0 mm for the cover placed on the inner metal surface, 8.0 mm × 6.0 mm placed on the inside and the external surface of the metal housing of the recorder), on the side plane (wall) of the cylinder (Fig. 5).

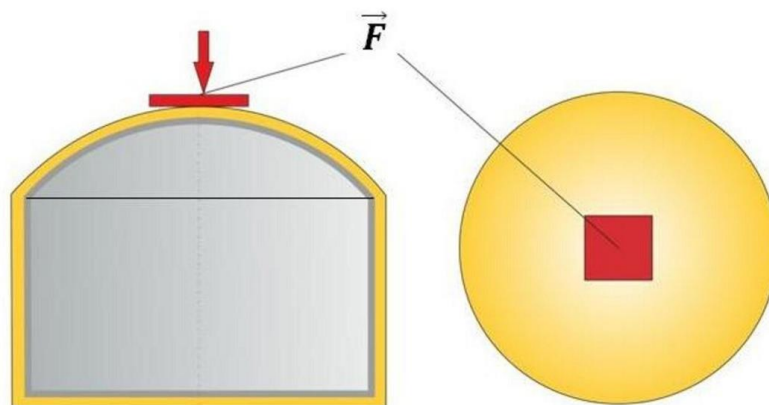


Figure 3. The load of the cover with concentrated force acting in the direction of the axis y .

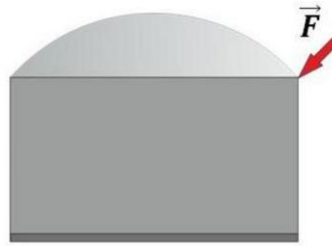


Figure 4. The load of the cover with concentrated force at an angle of 45°.

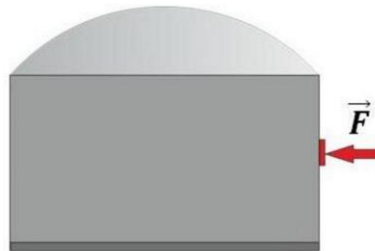


Figure 5. The load of the cover with concentrated force on the side plane (wall) of the cylinder.

In all cases, the adopted boundary conditions corresponded to the fixed groundwork of the model. In addition, a numerical analysis of dynamic tests was performed to determine the durability of the recorder. It consisted in dropping a weight of 227 kg, terminated with a properly shaped tip (width 0.65 cm), from a height of 3 m, onto the protective housing of the recorder, according to the most vulnerable for its damage load direction. In the case of this trial numerical calculations were carried out in the ANSYS Explicit Dynamics module, which allows simulation of dynamic conditions, e.g. for piercing the surface of composites. For this purpose, three three-dimensional models have been developed: weight, composite housing and rigid base, on which the housing is located (Fig. 6).

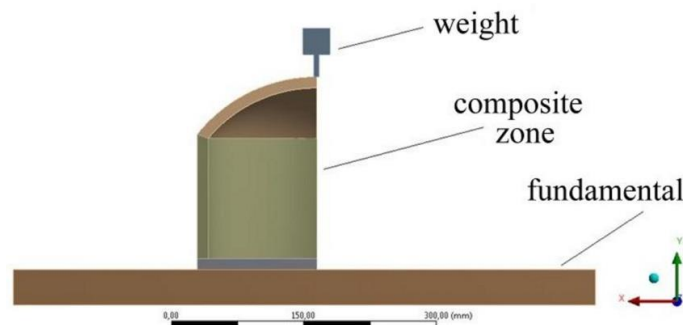


Figure 6. Numerical 3D model adopted for dynamic calculations for penetration of the composite zone.

The numerical model of the weight and the base has been assumed as a non-deformable element (rigid), made of steel with the Young's modulus of 200 GPa and a Poisson ratio of 0.3.

The composite zone was characterized by orthotropic properties and was treated as a deformable body. The models were divided into six-sided finite elements of the Hex8 type (Hexahedrons). The data presented in Table 4 were used for the calculations.

Table 4. Data accepted for calculating the durability of the recorder housing (Przybyłek, 2018).

| Parametr | Value |
|--|-------|
| The discharge height of the weight, (m) | 3.0 |
| Velocity adopted for calculations, (Value determined for ¼ of energy), (m/s) | 4.95 |

Due to the axial symmetry of the dome, the calculation was limited to its section, constituting $\frac{1}{4}$ of the whole (Fig. 7). For such a slice there is $\frac{1}{4}$ of the kinetic energy of the weight, what has been taken into account by reducing the speed accordingly. It allowed to shorten the calculation time.

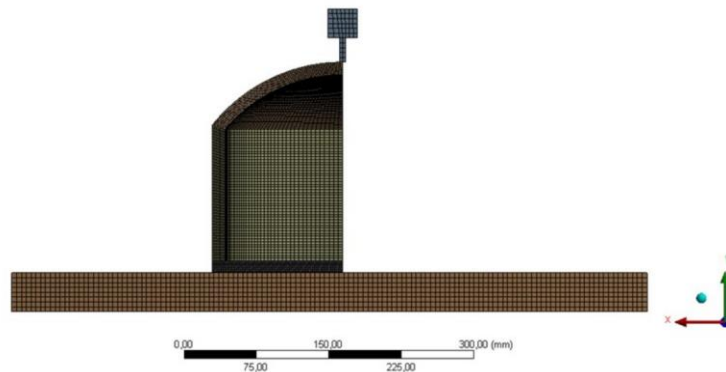


Figure 7. Division into finite elements of type Hex8 (Hexahedrons) of numerical models, accepted into calculation of dynamic resistance of composite sphere to puncture.

Modeled objects are in interaction, treated as a kind of contact (Body Interaction). It was assumed that the modeled base is rigid and immovable, without the possibility of moving in the direction of the x -axis and the z -axis.

3. Analysis of results

Based on the results obtained from numerical calculations, the adhesive strength of the joints was assessed. The displacements of the entire model and stress σ_x were analyzed that can cause delamination and stress τ_{yz} causing inter-layer shear. Results of stress calculations in all load cases and for all types of placement of the composite in correlation with the metal housing are presented in Tables 5 and 6.

Table 5. Maximum directional stresses of composite layers of the 3D model of cover 1, with division into load cases and the way of strengthening in MPa (Przybyłek, 2018).

| Cases | Maximum von Mises stresses (in the whole model) | Basis | | | | | | Cylinder | | | | | | Bowl | | | | | | |
|---|--|---|-------|-------------------|------------------------------|-------|-------------------|----------------------------|-------|-------------------|------------------------------|-------|-------------------|----------------------------|-------|-------------------|------------------------------|-------|-------------------|------|
| | | Maximum stress imposed on adhesive joints | | | | | | | | | | | | | | | | | | |
| | | Normal stresses σ_y | | | Contact stresses τ_{xz} | | | Normal stresses σ_x | | | Contact stresses τ_{yz} | | | Normal stresses σ_y | | | Contact stresses τ_{xz} | | | |
| | | Composite inside | Metal | Composite outside | Composite inside | Metal | Composite outside | Composite inside | Metal | Composite outside | Composite inside | Metal | Composite outside | Composite inside | Metal | Composite outside | Composite inside | Metal | Composite outside | |
| Composite cover | 1. | 120 | 0,46 | | 0,27 | | | 4,53 | | | 3,32 | | | 7,57 | | | 8,29 | | | |
| | 2. | 50,4 | 5,6 | | 2 | | | 19,3 | | | 13,5 | | | 7,8 | | | 9,8 | | | |
| | 3. | 334 | 37 | | 10,3 | | | 112,8 | | | 39,8 | | | 14,1 | | | 7,5 | | | |
| Composite cover + metal inside | 4. | 242 | - | 90 | 13 | - | 30,5 | 6 | - | 22 | 30 | - | 62 | 19 | - | 10 | 1,5 | - | 20 | 4,3 |
| | 5. | 45,6 | - | 5,7 | 2,3 | - | 14 | 1,9 | - | 4 | 14 | - | 12,7 | 12,3 | - | 2,8 | 5,3 | - | 10 | 0,87 |
| | 6. | 90,2 | - | 0,4 | 0,1 | - | 0,26 | 0,4 | - | 0,29 | 0,1 | - | 0,13 | 0,08 | - | 21,8 | 30 | - | 16,3 | 9,7 |
| Composite cover + metal outside | 1. | 492 | 0,12 | 1,12 | | 0,06 | 1,67 | | 0,3 | 1,19 | | 0,6 | 3,1 | | 53 | 91 | | 3,7 | 85 | |
| | 2. | 66,8 | 0,19 | 10,7 | | 0,34 | 5,03 | | 0,9 | 21,7 | | 0,8 | 24,4 | | 1,13 | 19 | | 0,28 | 17,5 | |
| | 3. | 814 | 4,8 | 101 | | 2,5 | 12,4 | | 5,9 | 153 | | 13 | 126 | | 2,3 | 25 | | 2,1 | 7,9 | |
| Metal+composite outer cover + composite inner cover | 1. | 238,9 | 0,21 | 0,75 | 0,05 | 0,16 | 1,65 | 0,1 | 0,16 | 1,76 | 1,16 | 0,63 | 1,76 | 0,59 | 0,88 | 5,06 | 5,39 | 3,83 | 54,79 | 4,38 |
| | 2. | 33,92 | 0,075 | 13,21 | 1,59 | 0,34 | 4,8 | 0,13 | 1,19 | 13,47 | 1,21 | 0,81 | 12,5 | 0,57 | 1,18 | 23,53 | 0,85 | 0,31 | 11,7 | 0,27 |
| | 3. | 873,5 | 7,7 | 46,52 | 21,02 | 3,35 | 18,98 | 1,12 | 9,48 | 16,48 | 162,8 | 15,48 | 135,2 | 30,53 | 3,9 | 40,39 | 6,8 | 2,79 | 19,82 | 1,71 |

Table 6. Maximum directional stresses of composite layers of the 3D model of cover 2, with division into load cases and the way of strengthening in MPa (Przybyłek, 2018).

| Cases | Maximum von Mises stresses (in the whole model) | Basis | | | | | | Cylinder | | | | | | Bowl | | | | | | | | |
|---|---|---|-------|-------------------|------------------------------|-------|-------------------|----------------------------|-------|-------------------|------------------------------|-------|-------------------|----------------------------|-------|-------------------|------------------------------|-------|-------------------|-------|-------|--|
| | | Maximum stress imposed on adhesive joints | | | | | | | | | | | | | | | | | | | | |
| | | Normal stresses σ_y | | | Contact stresses τ_{xz} | | | Normal stresses σ_x | | | Contact stresses τ_{yz} | | | Normal stresses σ_y | | | Contact stresses τ_{xz} | | | | | |
| | | Composite inside | Metal | Composite outside | Composite inside | Metal | Composite outside | Composite inside | Metal | Composite outside | Composite inside | Metal | Composite outside | Composite inside | Metal | Composite outside | Composite inside | Metal | Composite outside | | | |
| Composite cover | 1. | 119,5 | 0,62 | 0,62 | | | 0,38 | | | 5,31 | | | | | 3,87 | | | 29,79 | | | 10,11 | |
| | 2. | 60,83 | 0,23 | 7,05 | | | 2,67 | | | 24,71 | | | | | 16,2 | | | 9,43 | | | 11,67 | |
| | 3. | 464,3 | 1,51 | 57,79 | | | 6,012 | | | 230,2 | | | | | 41,05 | | | 12,41 | | | 7,78 | |
| Composite cover + metal inside | 1. | 202 | 0,34 | - | 63 | 13 | - | 16 | 1,4 | - | 23 | 16 | - | 66 | 5 | - | 9 | 3 | - | 6,4 | | |
| | 2. | 48 | 0,05 | - | 6 | 2,3 | - | 11 | 0,6 | - | 4,8 | 13 | - | 19 | 16 | - | 2,4 | 6,8 | - | 5 | | |
| | 3. | 130 | 0,26 | - | 0,9 | 0,05 | - | 0,4 | 0,13 | - | 4,5 | 0,28 | - | 4,1 | 0,6 | - | 7,8 | 19 | - | 46,8 | | |
| Composite cover + metal outside | 1. | 406,4 | 0,16 | 0,081 | 1,48 | | 0,08 | 1,82 | | 1,8 | 5,59 | | 1,59 | 7,2 | | 1,54 | 34,01 | | 3,29 | 93,32 | | |
| | 2. | 62,79 | 0,04 | 0,22 | 13,8 | | 0,42 | 5,93 | | 0,76 | 21,76 | | 0,89 | 23,14 | | 0,43 | 32,46 | | 0,57 | 17,04 | | |
| | 3. | 1080 | 0,36 | 4,81 | 122,3 | | 2,76 | 11,22 | | 13,17 | 199,7 | | 15,01 | 185,5 | | 0,41 | 48,13 | | 1,28 | 13,47 | | |
| Metal+composite outer cover + composite inner cover | 1. | 88,79 | 0,51 | 0,32 | 0,03 | 0,05 | 0,23 | 0,15 | 0,015 | 0,53 | 0,82 | 0,62 | 2,84 | 1,92 | 2,56 | 4,4 | 0,1 | 25,05 | 7,13 | 3,79 | | |
| | 2. | 83,05 | 0,053 | 0,3 | 6,38 | 3,18 | 0,69 | 9,08 | 0,94 | 0,83 | 4,98 | 19,42 | 1,18 | 17,06 | 20,5 | 1,42 | 9,36 | 11,13 | 0,34 | 6,26 | | |
| | 3. | 397,1 | 0,81 | 12,7 | 20,83 | 3,34 | 3,43 | 28,36 | 1,97 | 16,97 | 26,41 | 91,64 | 8,85 | 80,09 | 45,07 | 3,53 | 26,97 | 4,32 | 1,21 | 15,71 | | |

The use of numerical analysis also enables the development of graphical depiction of stress distributions in the universal cover of the recorder housing (Fig. 8 and 9).

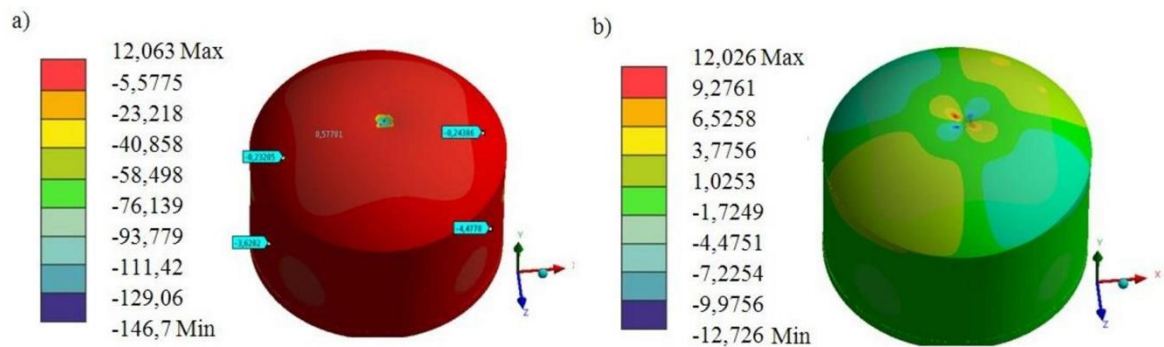


Figure 8. Stresses in the universal housing of the aircraft recorder, done from epoxy ablation composite, laden with concentrated force in the direction of the y axis (from the top): a) normal stresses that can cause delamination of σ_y , b) shear stresses that may cause inter-layer shear τ_{xz} .

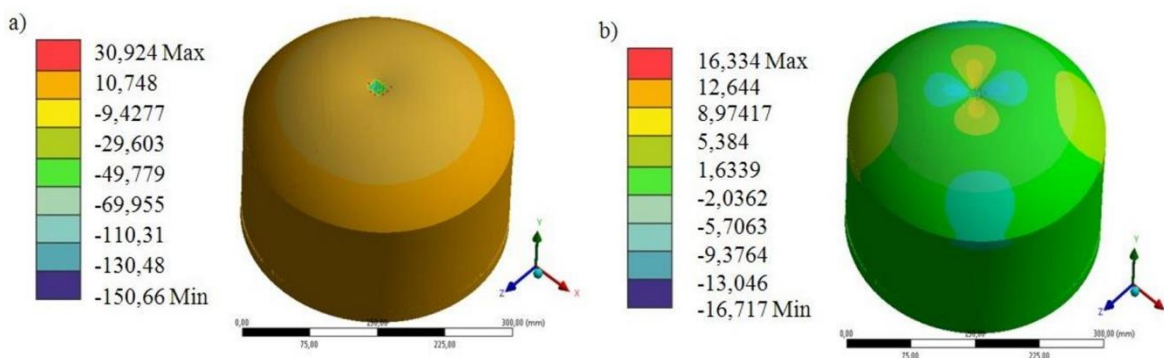


Figure 9. Stresses in the universal housing of the aircraft recorder, made of epoxy ablation composite, with metal housing placed inside the cover, laden with concentrated force in the direction of the y axis (from the top): a) normal stresses that can cause delamination of σ_y , b) shear stresses that may cause inter-layer shear τ_{xz} .

The model of the universal cover of the flight recorder also allows determination of the distribution of reduced stresses in individual layers of the cover material (Fig. 10).

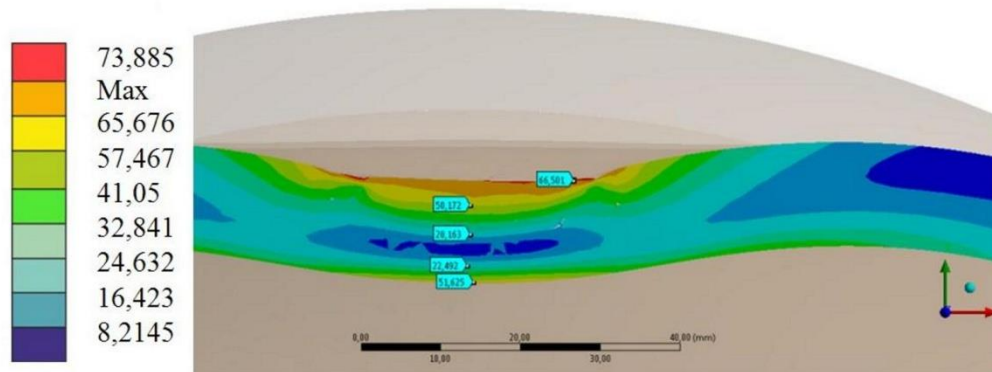


Figure 10. Stresses reduced in the composite material of the universal housing of the aircraft recorder, made of polymeric ablative composite, laden with concentrated force in the direction of the y axis (from the top).

Calculation of the maximum load in the whole model of the universal cover of the recorder (Tables 7 and 8).

Table 7. Maximum displacement in the whole model, cover 1 (Przybyłek, 2018).

| Cover 1 | | | | |
|--|-----------------|--------------------------------|--|---------------------------------|
| The way of charging | Composite cover | Composite cover + metal inside | Metal + outer composite cover + composite cover inside | Composite cover + metal outside |
| | | | | |
| Load with concentrated force applied on the side plane of the cylinder | 0.60 | 0.39 | 0.28 | 0.22 |
| Loading force concentrated on the node connecting the canopy with the cylinder pointing at an angle of 45° | 0.22 | 0.03 | 0.033 | 0.032 |
| Load with concentrated force directed along the y direction | 1.9 | 0.043 | 0.67 | 0.39 |

The distribution of kinetic and potential energy during piercing of the composite thermo-protective casing was determined by numerical simulation for the housing of recorder made of an epoxy ablation composite, with a metal layer located inside the casing.

Analysis of energy changes allows you to observe the reflection of the weight from the material of the spherical cap in 23 400 modeled load cycles for a composite shell (Fig. 11) and 33 650 modeled load cycles for the flight recorder cover made of a polymeric ablative composite with a metal casing placed inside (Fig. 12).

Table 8. Maximum displacement in the whole model, cover 2 (Przybyłek, 2018).

| Cover 2 | | | | |
|--|-----------------|--------------------------------|--|---------------------------------|
| The way of charging | Composite cover | Composite cover + metal inside | Metal + outer composite cover + composite cover inside | Composite cover + metal outside |
| | | | | |
| Load with concentrated force applied on the side plane of the cylinder | 0.62 | 0.34 | 0.51 | 0.16 |
| Loading force concentrated on the node connecting the canopy with the cylinder pointing at an angle of 45° | 0.23 | 0.05 | 0.053 | 0.04 |
| Load with concentrated force directed along the y direction | 1.51 | 0.26 | 0.81 | 0.04 |

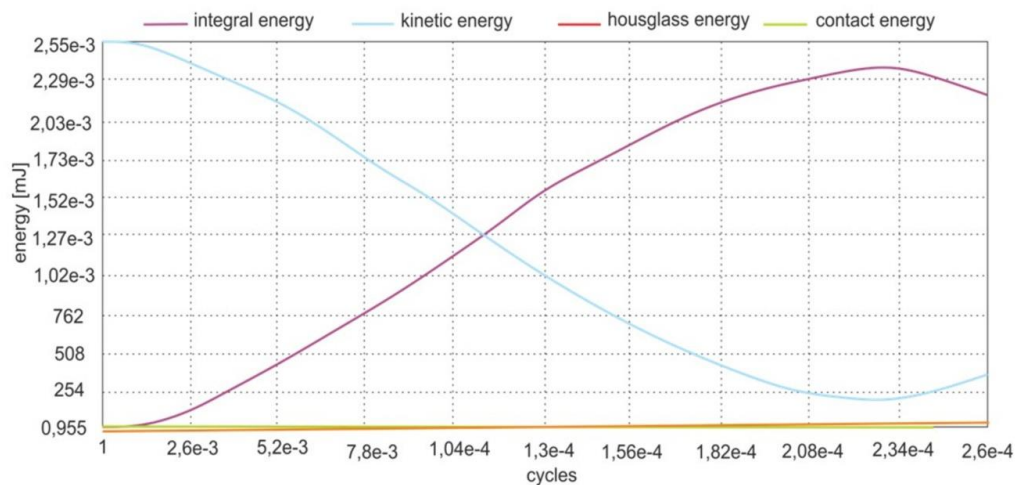


Figure 11. Graphs of potential energy changes during piercing (dark line) and kinetic energy (light line) universal composite thermo-protective cover (Przybyłek, 2018).

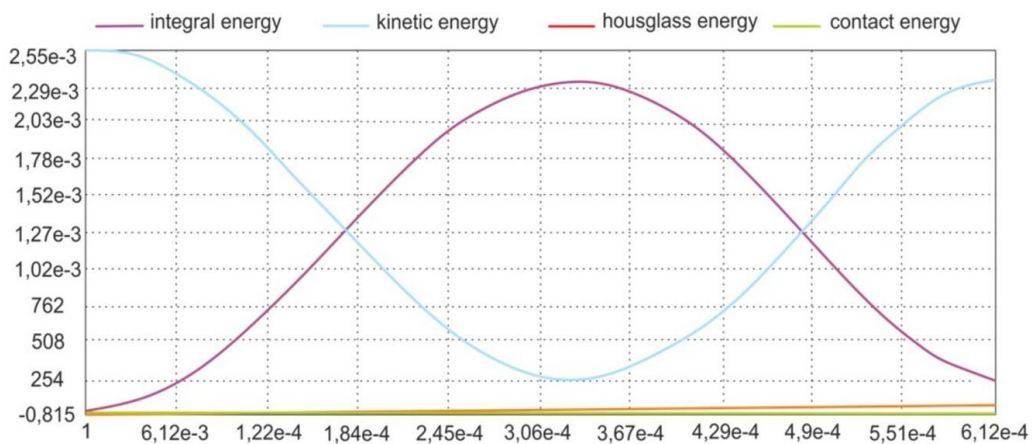


Figure 12. Graphs of potential energy changes during piercing (dark line) and kinetic energy (light line) recorder housing, made of polymer composite, with a metal layer inside the cover (Przybyłek, 2018).

Numerically obtained results in the form of maximum values of reduced stresses (von Misessa), shown in Figure 13, refer to the calculation results for a composite cover.

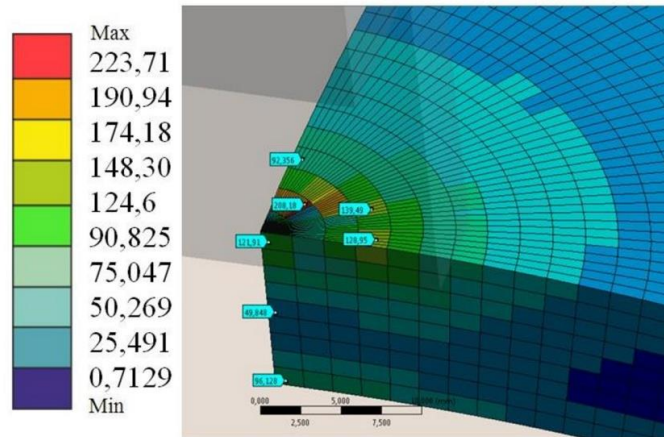


Figure 13. The average value of von Misess's stresses in the elements of the composite cover (Przybyłek, 2018).

Von Misess stresses, when trying to penetrate the composite cover, obtain the maximum value after time $t = 0.00036$ s (Fig. 14).

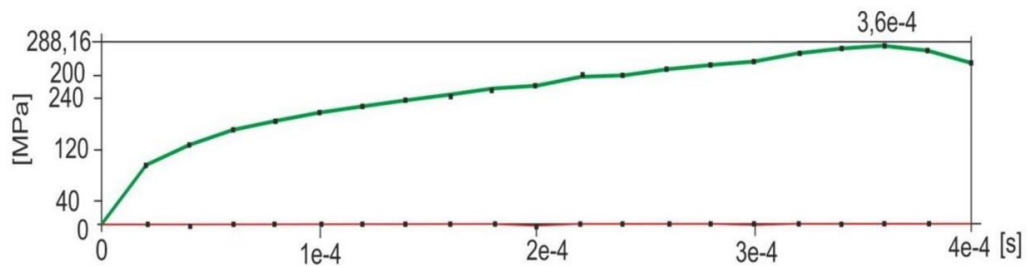


Figure 14. Graph of mean von Misessa stress values in cover elements, including the point ($t = 0.00036$ s), with the highest value of stresses during piercing (Przybyłek, 2018).

Changes in the energy and von Mises stress values during penetration of the composite shell show the process of the weight reflecting off the protective cover. Normal stress values in the direction of the y-axis are important for individual cases, as they suggest partial damage to the cover material (Fig. 15).

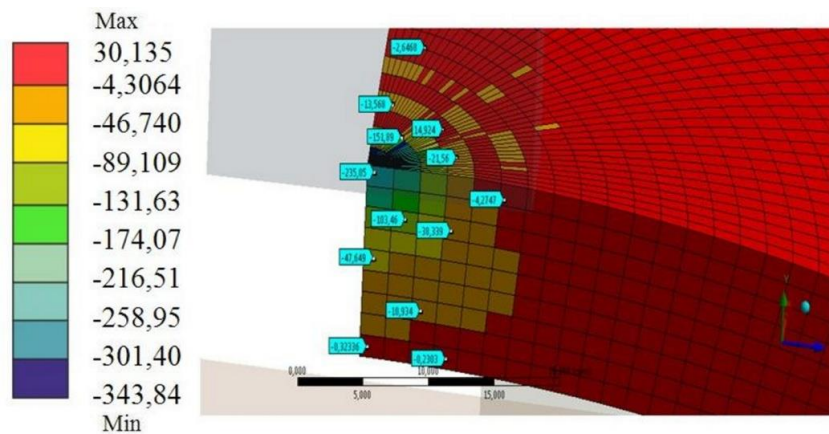


Figure 15. The average value of normal stresses in elements, in the direction of the y axis, which may cause delamination of the layers of the autonomous composite cover (Przybyłek, 2018).

There is an analogic observation in the case of shear stresses in the xz plane for a composite shell (Fig. 16) and for the housing of a recorder made of a polymeric ablative composite with a metal layer placed inside the cover. Stress values in the metal layer are negligible.

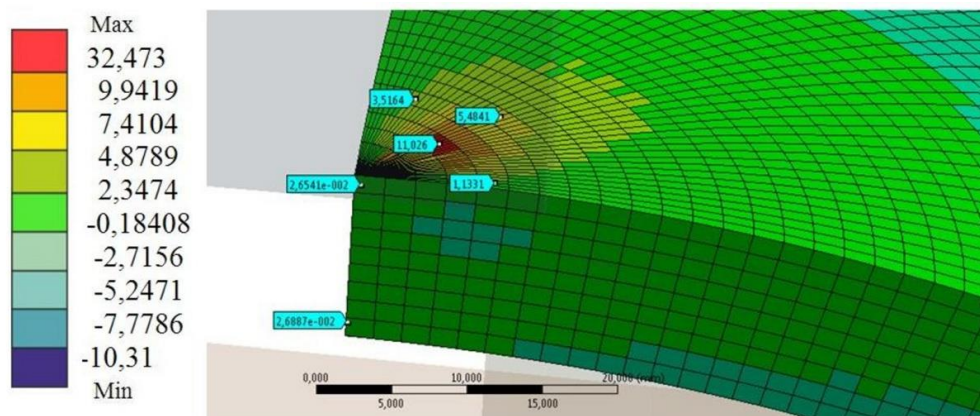


Figure 16. The average value of tangential stresses in the xz plane in elements of an autonomous composite shell, likely to cause inter-layer shear (Przybyłek, 2018).

4. Conclusions

The numerical analyses carried out are subject to uncertainty due to the inability to verify them with the experiment. However, they enable preliminary assessment of the considered types of placement of the composite cover in combination with the metal layer of the recorder. The influence of geometrical dimensions on the stress value σ_x was considered, which can cause delamination of the composite layers and τ_{yz} stresses that may cause inter-cutting shear.

Based on the analysis carried out, it can be concluded that the metal layer will not be damaged during breakthrough, while the composite layer will be partially damaged in both cases, which will reduce its thermo protective properties. In both cases the punch will be reflected from the tested structure. When loading a model reinforced with an inner metal layer, higher stresses in the composite can be observed compared to the second case. Results have been analyzed and conclusions have been made regarding the possibility of creating a real shield for the recorder, which will meet the normative requirements.

References

- ADAC warnt vor der Blackbox fürs Auto. (2015). <http://www.welt.de/motor/article108814877/ADAC-warnt-vor-der-Blackbox-fuers-Auto.html/> Accessed 19 March 2015.
- Alagar, M., Ashok K. A., Mahesh, K. P.O., & Dinakaran, K. (2000). Studies on thermal and morphological characteristics of E-glass/Kevlar 49 reinforced siliconized epoxy composites. *European Polymer Journal*, 36, 2449-2454. [http://dx.doi.org/10.1016/S0014-3057\(00\)00038-0](http://dx.doi.org/10.1016/S0014-3057(00)00038-0)
- Bahramian, A. R. (2013). Effect of external heat flux on the thermal diffusivity and ablation performance of carbon fiber reinforced novolac resin composite. *Iranian Polymer Journal*, 22, 579-589. <http://dx.doi.org/10.1007/s13726-013-0157-z>
- Bakar, M., Kucharczyk, W., & Stawarz, S. (2016). Investigation of thermal and ablative properties of modified epoxy resins. *Polymers & Polymer Composites*, 24(8), 617-623.
- Bieniaś, J., & Jakubczak, P. (2017). Impact damage growth in carbon fibre aluminium laminates. *Composite Structures*, 172, 147-154. <https://doi.org/10.1016/j.compstruct.2017.03.075>
- Camino, G., Tartaglione, G., Frache, A., Manfredi, C., & Costa, G. (2005). Thermal and combustion behaviour of layered silicate-epoxy nanocomposites. *Polymer Degradation and Stability*, 90, 354-362. <http://dx.doi.org/10.1016/j.polymdegradstab.2005.02.022>

- EUROCAE. (2013). Minimum Operational Performance Specification For Crash Protected Airborne Recorder Systems, Revision A.
- Fino, P., Lombardi, M., Antonini, A., Malucelli, G., & Montanaro, L. (2012). Exploring composites based on PPO blend as ablative thermal protection systems – Part II: The role of equiaxial fillers. *Composite Structures*, 94, 1060-1066. <http://dx.doi.org/10.1016/j.compstruct.2011.10.020>
- GM Automatic Crash Response System (ACR). (2016). <http://cms.cerritos.edu/auto/basic-its/ost.htm/> Accessed 13 September 2016.
- Haack, A. (2004). Latest achievements and perspectives in tunnel safety. Author's presentation 30nd ITA – World Tunnel Congress, Singapore, 22-27 May 2004.
- IEEE 1616-2004 - IEEE Standard for Motor Vehicle Event Data Recorder (MVEDR). (2004). IEEE – Institute of Electrical and Electronics Engineers. <http://standards.ieee.org/> Accessed 24 February 2012.
- Krzyżak, A., Kucharczyk, W., Gąska, J., & Szczepaniak, R. (2018). Ablative test of composites with epoxy resin and expanded perlite. *Composite Structures*, 202, 978-987. <http://dx.doi.org/10.1016/j.compstruct.2018.05.018>
- Kucharczyk, W. (2010). Some ablative properties of epoxy composites used for thermo-protection (in Polish). *Przemysł Chemiczny*, 89(12), 1673-1676.
- Kucharczyk, W., Dusiąski, D., Żurowski, W., & Gumiński, R. (2018). Effect of composition on ablative properties of epoxy composites modified with expanded perlite. *Composite Structures*, 183, 654-662. <http://dx.doi.org/10.1016/j.compstruct.2017.08.047>
- Kucharczyk, W., Przybyłek, P., & Opara, T. A. (2013). Investigation of the thermal protection ablative properties of thermosetting composites with powder fillers: the corundum Al₂O₃ and the carbon powder C. *Polish Journal of Chemical Technology*, 15(4), 49-53. <http://dx.doi.org/10.2478/pjct-2013-0067>
- Lombardi, M., Fino, P., Malucelli, G., & Montanaro, L. (2012). Exploring composites based on PPO blend as ablative thermal protection systems – Part I: The role of layered fillers. *Composite Structures*, 94, 1067-1074. <http://dx.doi.org/10.1016/j.compstruct.2011.10.019>
- Ministere des Transports, Bureau d'Enquêtes et d'Analyses pour la Sécurité de l'Aviation Civile. (2005). Flight Data Recorder Read-Out, Technical and Regulatory Aspects. https://www.bea.aero/uploads/tx_scalaetudessecurite/use.of.fdr_01.pdf Accessed 19 July 2020.
- Minkook, K., Jaeheon, C., & Dai, G. L. (2016). Development of the fire-retardant sandwich structure using an aramid/glass hybrid composite and a phenolic foam-filled honeycomb. *Composite Structures*, 158, 227-234. <http://dx.doi.org/10.1016/j.compstruct.2016.09.029>
- NIST NCSTAR 1. (2005). Final report on the Collapse of the World Trade Center. Washington: U.S. Government Printing Office.
- Ono, K., & Otsuka, T. (2006). Fire design requirement for various tunnel. Authors' presentation of 32nd ITA – World Tunnel Congress, Seoul, 25 April 2006.
- Polak, Z., & Rypulak, A. (2002). Avionics instruments and on-board systems (in Polish). Dęblin: Polish Air Force Academy.
- Przybyłek, P. (2018). Analysis of possibilities to improve thermal resistance assessment of the universal flight data recorder by application of shield, made with polymer ablative composites (in Polish). Unpublished Doctoral Dissertation. Radom: Kazimierz Pulaski University of Technology and Humanities in Radom.
- Przybyłek, P., & Opara, T. A. (2010). Flight data recorders, protective case. *Journal of Aeronautica Integra*, 8(2), 43-50.
- Pulci, G., Tirillň, J., Marra, F., Fossati, F., Bartuli, C., & Valente, T. (2010). Carbon–phenolic ablative materials for re-entry space vehicles: Manufacturing and properties. *Composites: Part A*, 41, 1483-1490. <http://dx.doi.org/10.1016/j.compositesa.2010.06.010>
- Rallini, M., Puri, I., Torre, L., & Natali, N. (2018). Boron based fillers as char enhancers of EPDM based heat shielding materials for SRMs: A comparative analysis. *Composite Structures*, 198, 73-83. <https://doi.org/10.1016/j.compstruct.2018.03.102>

Ryabov, A., Romanov, V., Kukanov, S., & Roschihmarow, D. (2003). Numerical simulation of flight data recorder's protective case penetration resistance test. 4th European L-S DYNA Users Conference, Ulm.

Shi, S., Wang, Y., Yan, L., Sun, P., Li, M., & Tang, S. (2020). Coupled ablation and thermal behavior of an all-composite structurally integrated thermal protection system: Fabrication and modeling. *Composite Structures*, 251, 112623. <https://doi.org/10.1016/j.compstruct.2020.112623>

Stawarz, S., Witek, N., Kucharczyk, W., Bakar, M., & Stawarz, M. (2019). Thermo-protective properties of polymer composites with nano-titanium dioxide. *International Journal of Mechanics and Materials in Design*, 15(3), 585-599. <http://dx.doi.org/10.1007/s10999-018-9432-7>

U.S. Department Of Transportation, National Highway Traffic Safety Administration – NHTSA. (2010). Event Data Recorders. 49 CFR Part 563, Docket No. NHTSA-2004-18029. <http://www.nhtsa.gov/Laws+&+Regulations/Other+Equipment/> Accessed 15 February 2010.

U.S. Department Of Transportation, National Highway Traffic Safety Administration – NHTSA. (2015). Event Data Recorder (EDR) Research Applications of Articles, Products and Research. <http://www.nhtsa.gov/EDR/> Accessed 23 October 2016.

Wilkinson, T. (2002). The World Trade Center and 9/11: The discussion of some engineering design issues. National Conference “Safe Buildings for This Century”. Australian Institute of Building Surveyors, Sydney.

Yuan, W., Wang, J., Song, H., Ma, T., Wu, W., Li, J., & Huang, C.H. (2018). High-power laser resistance of filled sandwich panel with truss core: An experimental study. *Composite Structures*, 193, 53-62. <https://doi.org/10.1016/j.compstruct.2018.03.031>

Zhou, L. Ch., Sun, X. H., Chen, M. W., Zhu, Y. B., & Wu, H. A. (2019). Multiscale modeling and theoretical prediction for the thermal conductivity of porous plain-woven carbonized silica/phenolic composites. *Composite Structures*, 215, 278-288. <https://doi.org/10.1016/j.compstruct.2019.02.053>.

[dataset] (2011). 14 CFR § 121.344 - Digital flight data recorders for transport category airplanes, 1 January. <https://www.govinfo.gov/app/details/CFR-2011-title14-vol3/CFR-2011-title14-vol3-sec121-344/summary/> Accessed 19 July 2020.